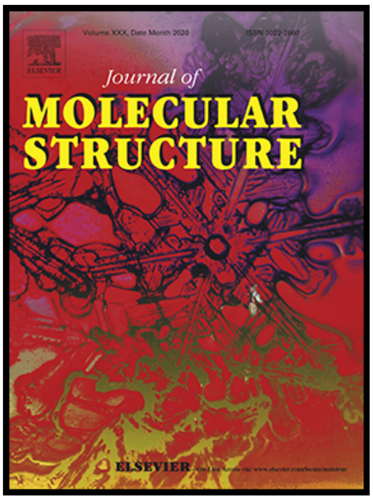

A novel organic reaction leading to new 2-N-substituted benzoic acid ion-pair. A combination of physicochemical and theoretical Calculations approaches

Abir. Ben Hadj Amor , Sameh. Akriche , Youssef. Arfaoui , Raoudha. Abderrahim

PII: S0022-2860(20)31246-1
DOI: https://doi.org/10.1016/j.molstruc.2020.128921
Reference: MOLSTR 128921

To appear in: *Journal of Molecular Structure*

Received date: 24 March 2020
Revised date: 13 July 2020
Accepted date: 15 July 2020

Please cite this article as: Abir. Ben Hadj Amor , Sameh. Akriche , Youssef. Arfaoui , Raoudha. Abderrahim , A novel organic reaction leading to new 2-N-substituted benzoic acid ion-pair. A combination of physicochemical and theoretical Calculations approaches, *Journal of Molecular Structure* (2020), doi: https://doi.org/10.1016/j.molstruc.2020.128921

Highlights

- Novel 2-aminobenzimidazole (ABZ)-2-N-propanoyl benzoic acid was synthesized.
- The structure of **1** was established by X-Ray crystallography.
- NBO analysis was carried out in order to obtain information on the electronic structure of **1**.
- Fukui function is used to interpret the mechanism of the formation of **1**.

A novel organic reaction leading to new 2-N-substituted benzoic acid ion-pair. A combination of physicochemical and theoretical Calculations approaches.

Abir. Ben Hadj Amor [a], Sameh. Akriche [b], Youssef. Arfaoui[c] and Raoudha. Abderrahim* [d]

a: Department of Chemistry. Faculty of Sciences of Bizerte, University of Carthage, 7021 Zarzouna, Bizerte, Tunisia

b: Laboratory of Material Chemistry. Faculty of Sciences of Bizerte, University of Carthage, 7021 Zarzouna, Bizerte, Tunisia

c: Laboratory of Characterizations, Applications & Modeling of Materials (LR18ES08), Department of Chemistry, Faculty of Sciences, University of Tunis El Manar, 2092, Tunis, Tunisia

d : Laboratory of Physics of Lamellaires Materials and Hybrids Nanomaterials, University of Carthage, Faculty of Sciences of Bizerte, Zarzouna 7021, Bizerte, Tunisia.

*Corresponding author: email: abderrahim75.raoudha@gmail.com

Abstract :

The 2-aminobenzimidazole (ABZ)-2-N-propanoyl benzoic acid **1** which is an intermediate of synthesis of various heterocyclic compounds was synthesized. The structure of **1** was confirmed by FT-IR, NMR (1D and 2D) spectra and XRD. The molecular structure of compound **1** was characterized by single-crystal X-ray structure determination and theoretical calculations based on DFT, HF and MP2 methods. The NBO analysis was used mainly in order to study the influence of electronic delocalization on the mechanism. Experimental, DFT, HF and MP2/6-31G(d) optimized bond lengths, bond angles and hydrogen bonding for the structure are studied also.

The structure analysis shows that the 3D-supramolecular architecture of **1** is stabilized by means six-(S6) intramolecular and eight-(R_2^2(8)) membered intermolecular hydrogen bonds, together with extensive C—H…O and C—H…π interactions between the carboxylate anion and the 2-aminobenzimidazolium cation. Furthermore, parameters derived from density functional theory in a local sense, in particular the softness and Fukui function were used to interpret and predict the mechanism of the reaction.

Key words: 2-N-propanoyl anthranilic acid, charge transfer complex, spectroscopic study, X ray diffraction analysis. Theoretical calculations.

1.Introduction

Benzimidazoles derivatives attract the attention of researchers [1]. This is due to their similarity to guanine and adenine DNA bases. Benzimidazole moiety is present in several pharmaceutical compounds. In the last years, this class of compounds has been reported to have anti-hypertensive anti-allergic, anti-diabetic, anti-inflammatory, mycobacterium, anti-oxidant, anti-protozoal, anti-viral and antimicrobial properties [2–8]. Compounds containing a benzimidazole moiety are important chemical classes due to their significant biological activities against several viruses such as HIV, herpes (HSV-1), influenza, Epstein-Barr and Burkitt's lymphoma promotion [9−11]. Moreover, benzimidazole derivatives have been studied as anticancer and antiproliferative chemicals [12,13]. The researchers are now interested to explore their potential as anti-cancer agents, an effort was made to further explore this area of research. The mechanism that has the most for anticancer action depends on strong metal ligand binding via the N atoms [14]. Furthermore, in order to increase the solubility and efficacy of these heterocycles, the interest is now shifted to the salts of these compounds. The complex were formed by non covalent intermolecular interactions that are especialy crucial to explain how molecules interconnect to form biological entity[15].

Alternatively, the placement of the N atoms in this molecule also makes it suitable for association with carboxylic acids, and four subsequent crystal structures have been reported [16-18]. In this research we are interested in anthranilic acid and it's reactivity. It has been shown that anthranilic acid derivatives have good antibacterial activity against several Gram-positive strains. *N*-acetylanthranilic acid is present as part of the structure of certain synthetic drugs such as the sedative methaqualone [19] and controlled in table I licit in drug and plastic production and react as inhibitors of replication protein A [20]. Charge transfer complexes have attracted a lot of attention in recent years [21-23]. They find applications in solar cells due to their high electrical conductivity [24- 26] and were obtained by several methods such as accessing mechanochemistry [27]. However the charge transfer complex are used as Furan Fragmentation Induced by Collisions with Low-Energy Helium Cations [28].

The first aim of the work is to synthesize the quinazoline but we obtained the compound 1. In general, the action of the orthoester on anthranilic acid leads to oxazine[29] which must react with the amines in two different way to give either quinazolines or N-acylanthranilic amide [30]. But in this work neither quinazoline nor N-acylanthranilic amide were obtained But we obtain the compound **1**

In this paper we report the synthesis, spectroscopic characterization and structure determination of the new molecular complex of 2-aminobenzimidazole and 2-N-propanoyl benzoic acid. In order to explain the mechanism of the formation of the title compound **1** and to confirm its structure, single crystal structure X-ray diffraction analysis and theoretical calculations such as DFT, HF and MP2 methods were employed for the structural characterization. NBO analysis was performed mainly to study the influence of electronic delocalization on the mechanism.

2.Experimental and computational procedures

2.1 Synthesis of the 2-aminobenzimidazole-2-N-propanoylanthranilic (benzoic) acid 1.

The 2-N-propanoylaminobenzoic acid was synthesized by a new method: when we treated the anthranilic acid with orthoester and used acetic acid as catalyst. When the reflux is complete, the reaction mixture is allowed to cool to room temperature and the solvent is removed the obtained product **2** (the 2-N-propanoyl anthranilic acid) is filtered and then recrystallized. The 2-aminobenzimidazole-2-N-propanoyle anthranilic acid **1** was prepared by heating under reflux of toluene in stoichiometric quantity of 2-N-propanonyl anthranilic acid **2** with 2-amino [1,2a] benzimidazole (ABZ) for 24h. After cooling to room temperature, the title product got precipitated out, which was filtered, washed with ether , dried and recrystallized from MeOH. The single crystal suitable for X-ray measurement was obtained by several recrystallizations in MeOH. Scheme.1 represents the reaction for the formation of the title compound **1**.

The compound **1** was obtained with good yield (70%). Mp = 270 °C. Elemental analysis calculated for ($C_{17}H_{18}N_4O_3$): %C : 62.57, %H : 5.52, %N: 17.17. Elemental analysis found:

% C : 62.56, % H : 5.53, %N: 17.16. The stoichiometry of the **1** was confirmed by elemental analysis that show that the complex has 1:1 stoichiometric ratio. The proton and the carbon groups related to the chemical shifts were shown in **Tables .2.**

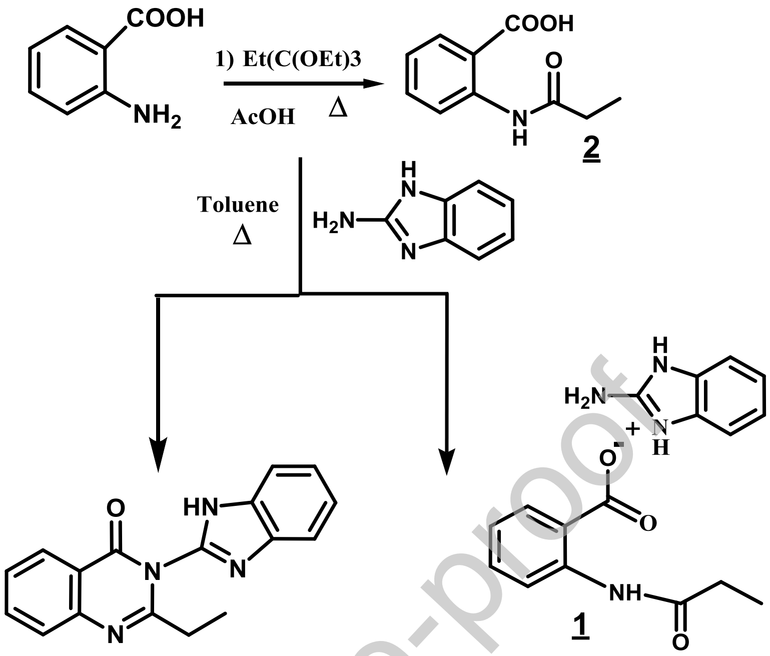

Scheme 1: Reaction scheme of synthesis of compound 1.

2.2.Infrared, NMR and Crystallographic characterization

IR spectra were recorded on a Nicolet TR 200 FT-IR spectrometer. Spectra resolution was 4 cm^{-1}. ^{1}H NMR and ^{13}C NMR spectra were recorded with the mixture $CDCl_3$-DMSO-d_6 as a solvent containing TMS (tetramethylsilane), on a Bruker 300 spectrometer (^{1}H: 300 MHz, ^{13}C: 75.47 MHz). The chemical shifts (δ) are reported in ppm relative to TMS (internal reference). For the ^{1}H NMR, the multiplicities of the signals are indicated for ^{1}H NMR using the following abbreviations: s: singlet, d: doublet, t: triplet, q: quartet, m: multiplet.

Melting points were obtained using a Büchi melting point apparatus and are uncorrected

X-ray diffraction measurements were recorded at 293 K temperature on Enraf Nonius Mach III X-ray diffractometer using K(α) (Ag), radiation ($\lambda = 0.5608$A°). The C, N, O atoms were obtained by direct method and the H atoms were obtained by the geometric calculation. The structures were solved by direct methods using the program SHELXS [31] and refined on F^2 by full matrix least squares method using SHELXL-97 [31]. Detailed crystallographic information is included in supporting information.

2.3.Computational methods

All calculations were performed with the GAUSSIAN-09 program [32]. The geometry optimizations for the title salt were carried out at the DFT, HF and MP2 levels of theory using the 6-31G(d) basis set, which includes one set of d polarization functions on the carbon, nitrogen and oxygen atoms. The B3LYP (Becke three parameter Lee–Yang–Parr exchange correlation functional are employed in the DFT studies, which combines the hybrid exchange functional of Becke [33] with the gradient correlation functional of Lee, Yang and Parr [34]. Starting geometries were taken from X-ray refinement data. Also, to investigate the stability, molecular properties such as highest molecular orbital (HOMO) and lowest molecular orbital (LUMO) energies, and the chemical hardness of the title compound are evaluated at B3LYP/6-31G(d) level of theory in gas phase.

To obtain more information on the electronic structures of stationary points, natural bond orbital (NBO), analysis was carried out. From density theory, it was possible to define and justify concepts of chemical reactivity such as the electronic chemical potential (μ), the absolute hardness (η), the global electrophilicity (ω) and the global softness (S) [35-37]. In practice, the condensed Fukui functions (f_k) at the atom k are usually evaluated from differences in atomic charges:

$f_k^+ = q_k(N+1) - q_k(N)$ (1) $f_k^- = q_k(N) - q_k(N-1)$ (2)

where q_k is the electronic charge of atom k and N is the number of electrons [37]. The two condensed Fukui functions f_k^+ and f_k^- characterize the reactivity preferences of nucleophilic and electrophilic attacks, respectively. In general, the greater value of a condensed Fukui functions, increases the reactivity of the corresponding atom.

3.Results and discussion

3.1.Spectroscopic data

The structure of complex **<u>1</u>** is investigated in detail by FT-IR, ^{1}H, ^{13}C NMR, DEPT, COSY, ^{13}C-^{1}H NMR HMQCGP, HMBCGP spectrometry.

3.1.1.Infrared spectra

Comparing the IR spectra of the complex **<u>1</u>** with the spectra of free ligands elucidated the mode of binding of the complex **<u>1</u>(Fig. 1)**. An infrared spectrum of the complex was recorded to confirm its structure. The vibration frequencies and their tentative assignments for 2-aminobenzimidazole and 2-N-propanonyl anthranilic acid ligands <u>2</u> and the complex **<u>1</u>** are listed in **Table 1**. The C=O is formed by π – π bonding between carbon and oxygen atoms.

The IR spectra of the complex showed characteristic bands due to the C=N group, symmetric and asymmetric stretching frequencies of NH, NH_2 and CO (acid and amide) functional groups of 2-aminobenzimidazole part, 2-N-propanonyl anthranilic acid moieties (Table.1).

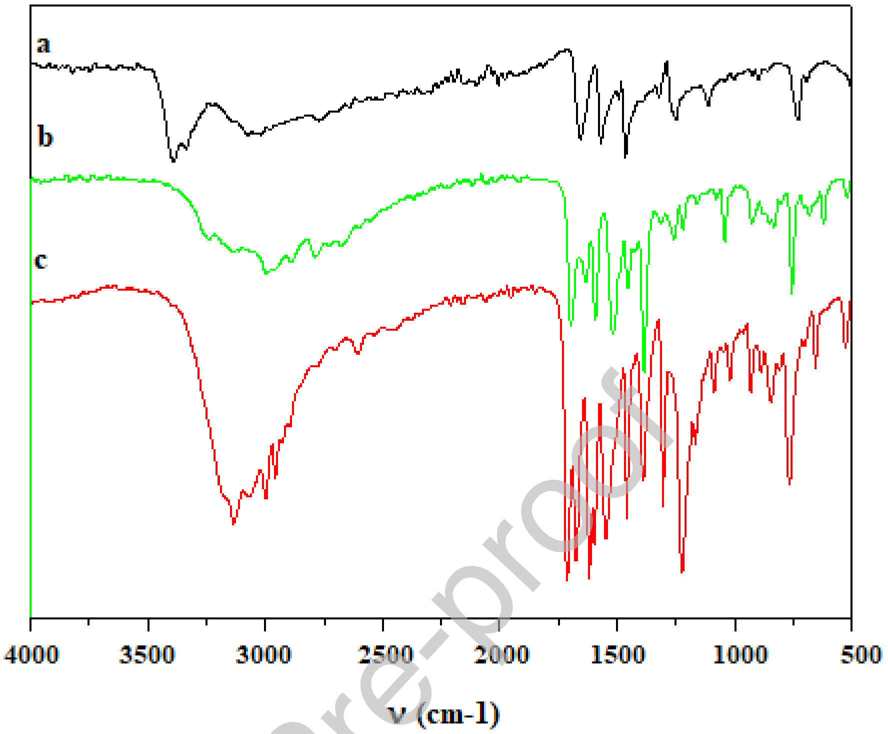

Figure.1: FT-IR of a) 2-aminobenzimidazole, b) complex **1** and c) 2-N-propanonyl anthranilic acid **2**.

Compound	IR data (cm^{-1}) assignements					
	ν (OH)	ν (NH)	ν (C=N)	ν (C=O)amide	ν(C=O) acid	ν (C=C)
Complex **1**		3240 3140	1637 1517	1637	1701	1594
Benzimidazole		3387 3310 3055	1651 1558			
Compound **2**	2998-3300	3109		1674	1712	1596

Table 1: The vibration frequencies assignements of **1**, ABZ and amide **2.**

The IR spectrum of 1 show the disappearance of the OH vibration. Then the NH and NH^{+} stretching vibration for the complex appears in the region of 3240–3140 cm^{-1} compared to the NH stretching wavenumbers of ABZ and Anthranilic amide as starting materials at 3055 and 3109 respectively. The bands in the spectrum (b)at 1637 is due to the bending vibrations of the group amide.

3.1.2.NMR spectra

The ^{1}H NMR spectra of the complex displayed signals due to both the donor and acceptor moiety with the appropriate shifts. ^{1}H NMR spectrum of the compound **2 (Fig.2a)**, and the compound **1** **(Fig.2b**). The spectrum of **1** show the disappearance of the signal at 9.95ppm corresponding to the proton of OH which indicated the proton transfer to the donor moiety. The signal at 7.80 ppm is assigned to NH_2. New peak appeared at 12.75 ppm in the complex indicate the presence of NH+.

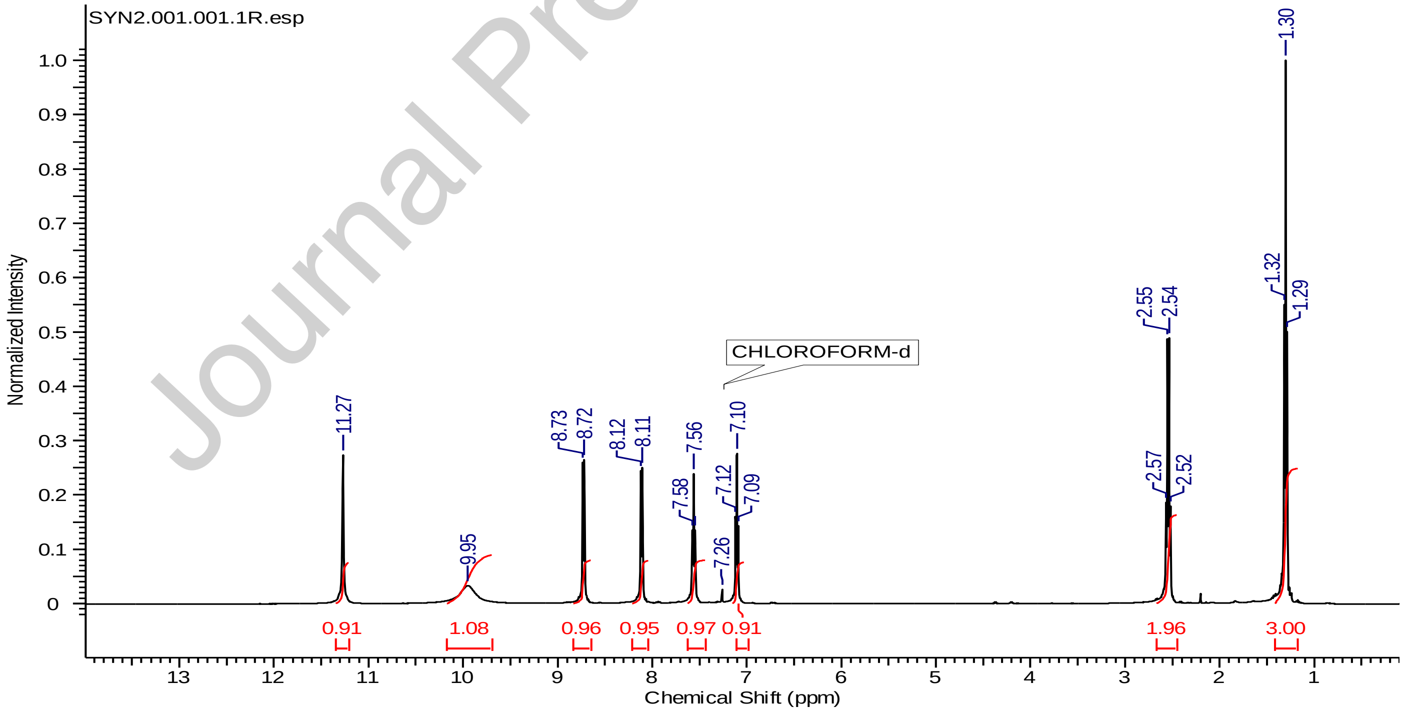

Figure 2a: Spectra of compound **2** in $CDCl_3$.

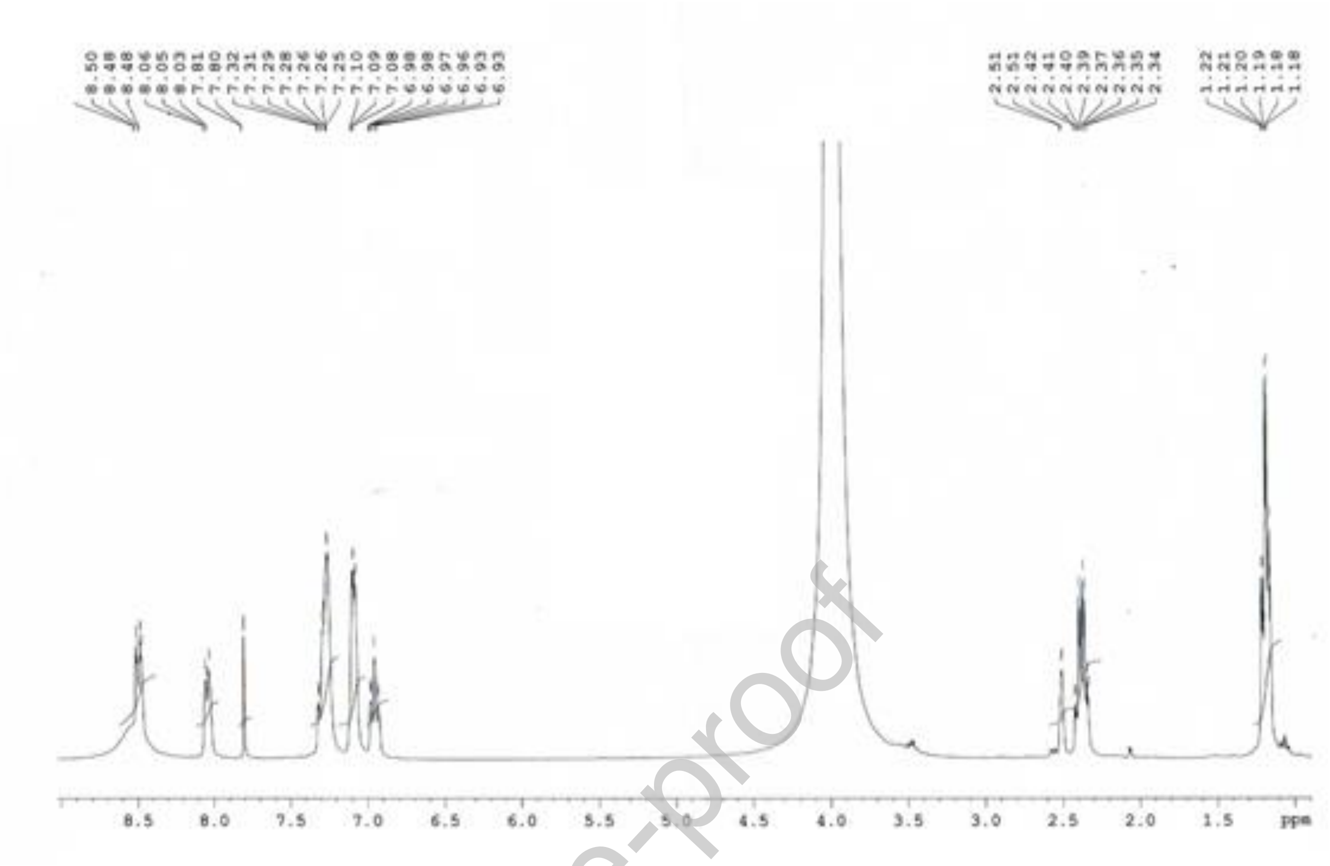

Figure. 2b : Spread spectra of **1** in DMSO d6.

The ^{13}C NMR spectra **(Fig.3)** of 2-N-propanonyl anthranilic acid and compound **1** spectra (Figure 3) confirm their formation. The experimental ^{13}C NMR and ^{1}H NMR chemical shifts are tabulated in Table 2.

The DEPT spectrum of **1** gives peaks at 31.11 ppm. It can be seen that there is one CH_3 and at 17.30 ppm in the DEPT spectrum.

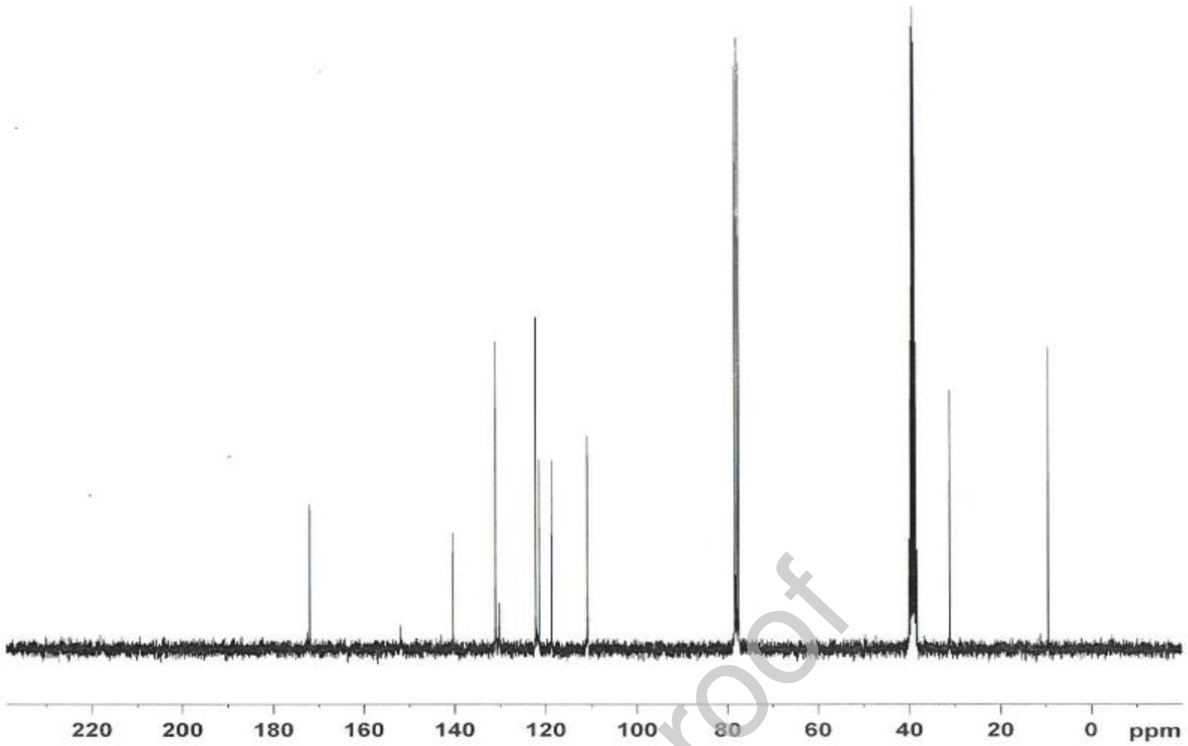

Figure 3: ^{13}C NMR Spectra of **1** in DMSO d6.

	^{1}H NMR data (ppm)	^{13}C NMR data (ppm)
Complex **1**		
	12.75 [bs, 2H, (NH, NH^+)]$_{ABZ}$	
		9.40 (CH_3)
	7.8 [s,1H (NH)]$_{Amide}$	31.11 (CH_2)
	6.8-8.5 [m,2{4H (C_6H_4)}]	110.87-140.40 [2(C_6H_4)]
	7.8 [2H (NH_2)]$_{ABZ}$	151.90(C=N)$_{ABZ}$
	2.4 [q, 2H (CH_2)]	172.02 [2(C=O)]
	1.20 [t, 3H (CH_3)]	
ABZ		
	10.83[1H (NH)]	
	7.12 [m,2H (C_6H_4)]	
	6.87 [m,2H (C_6H_4)]	
	6.15 [bs, 2H (NH_2)]	
2-N-propanonyl anthranilic acid		
	11.27 [s, 1H (OH)]	9.56 (CH_3)
	9.95 [s, 1H (NH)]	31.56 (CH_2)
	7.09-8.73 [m, 4H (C_6H_4)]	114.76-141.41 (C_6H_4)
	2.55 [q, 2H (CH_2)]	171.51(C=O)$_{amide}$
	1.30 [t,3H (CH_3)]	174.07(C=O)$_{acid}$

Table .2 : ^{1} H NMR and ^{13}C NMR assignments of chemical shifts of 1, ABZ and 2.

Assignments of the protons and carbons are also made by two-dimensional homonuclear and heteronuclear correlated experiments. The COSY spectrum shows the presence of the correlation between the H1, of ethyl with the H (arom) of benzimidazole moiety. The diagonal peaks serve only as reference points. The COSY spectrum of the salt shows the presence of the correlation between, the protons of the methyl groups (CH_3) with the methylene proton (CH_2) of ethyl. We can also see correlation between the aromatic protons. The H(3) and H(9) do not show off-diagonal peaks because those protons are not coupled to other protons in the molecule.

From HMQCGP spectra shown in figure 4, we notice that the peaks at 7.8 and 12.75 ppm in the proton spectrum have no correlations to the carbon spectrum. These are amine protons, the carbon peak at 110.87 ppm and the protons multiplet at 7.4 ppm correspond respectively to the aromatic carbons C_{14}, C_{15} and protons H_{11}; H_{12}. The carbon peak at 118.71 ppm and the protons multiplet at 8.5 ppm correspond to the aromatic carbons C_{13}, C_{16} and protons H_{10}; H_{13}.

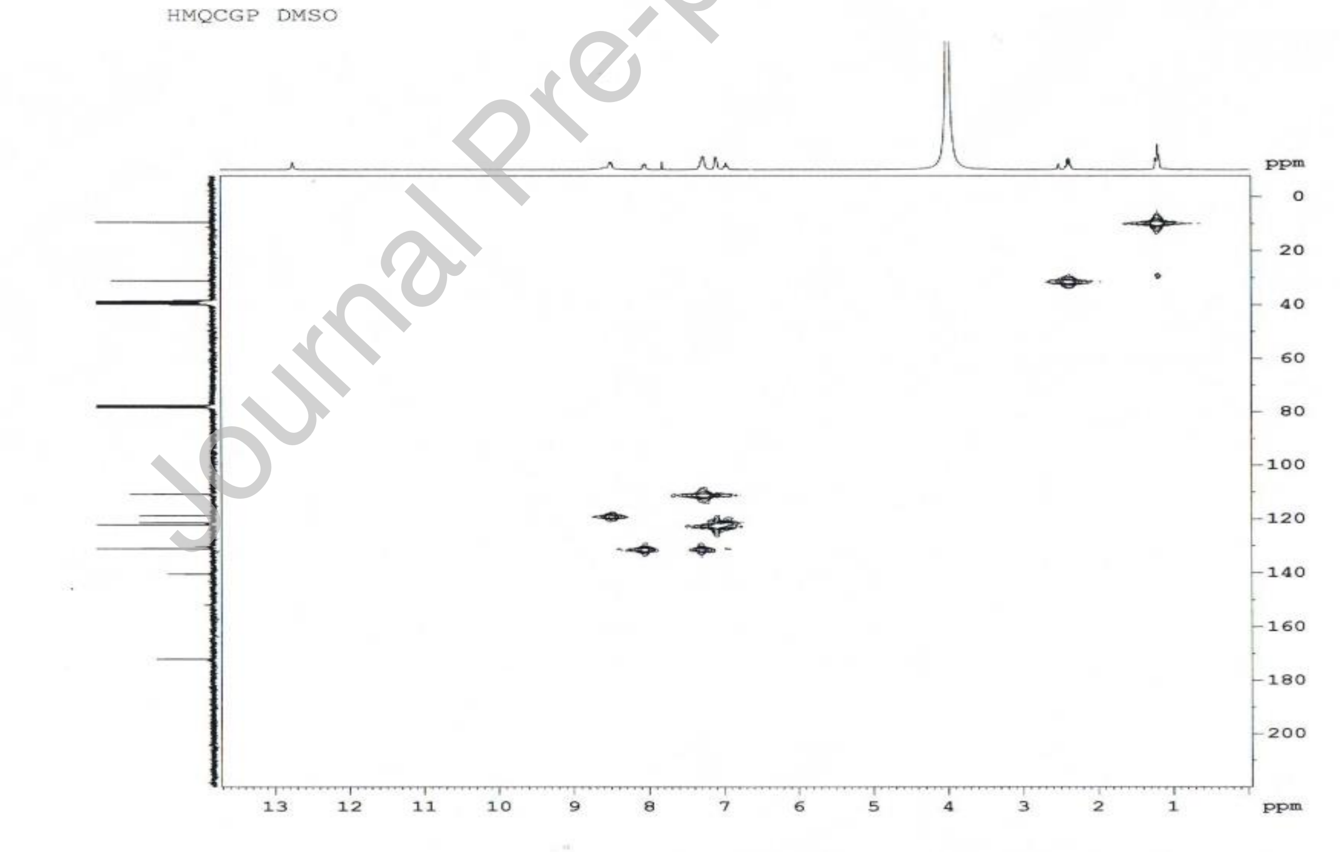

Figure 4: ^{13}C-^{1}H NMR HMQCGP spectra of **1.**

3.2.X-ray powder diffractometry

The Powder X-ray diffraction patterns of : a) complex **1**, b) 2-N-propanonyl anthranilic acid **2** and c) ABZ were presented in figure 5. The formation of the **1** was confirmed by X-ray diffractometry because there is a difference between the spectra of **1** and the spectra of 2-2-N-propanonyl anthranilic acid and ABZ spectra. So the powder X-ray diffraction of 1 revealed its cristallinity**.**

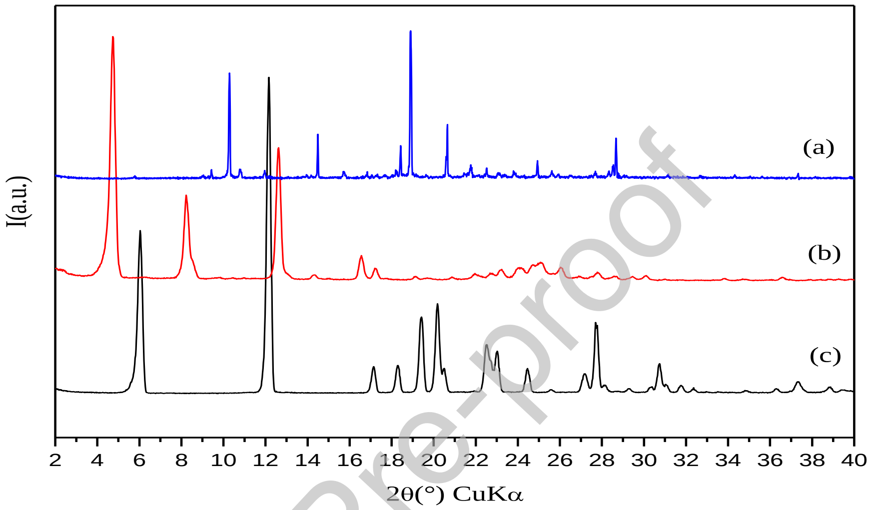

Figure. 5: Powder X-ray diffractometry of **(a).** Compound **1. (b)** 2-N-propanonyl anthranilic acid **2** . **(c)** ABZ

3.3.Crystal structure

Complex **1** consists of two distinct molecular moieties, a $C_7H_8N_3^+$ cation and a $C_{10}H_{10}NO_3^-$ anion (Fig. 6). As shown in figure 6, these molecular moieties are linked by means a multiple inter and intra molecular H-bonds occurring between the nitrogen atoms of cation and the oxygen atoms of anion. In fact, the asymmetric unit is stabilized by six and eight-membered intra and intermolecular hydrogen bonds corresponding to graph-set motifs of S(6) and R_2^2(8) respectively[31]. The S(6) intramolecular hydrogen bond is observed between the –NH and –CO groups of the anion, while the R_2^2(8) intermolecular hydrogen bond is observed between the --NH_2 and –NH groups of cation and the --CO_2^- group of anion. In addition to S(6) intramolecular hydrogen bond, two weak C—H…O interactions are also observed (Fig. 6). The hydrogen-bond parameters are listed in Table 3

Hydrogen-bond geometry (Å, °)

D—H···*A*	*D*—H	H···*A*	*D*···*A*	*D*—H···*A*
Intermolecular Interactions				
Graph set $R_2^2(8)$				
N1—H1*A*···O2	0.86	1.94	2.764 (4)	161
N2—H2···O1	0.86	1.90	2.756 (3)	172
Graph set association				
N1—H1*B*···O1^{i}	0.86	2.06	2.830 (3)	149
N3—H3*A*···O3^{ii}	0.86	1.89	2.722 (3)	164
C3—H3···O3^{iii}	0.93	2.56	3.425 (4)	155
Intramolecular Interactions				
N4—H4*A*···O2	0.86	1.91	2.591 (3)	135
C11—H11···O3	0.93	2.33	2.892 (4)	118
C14—H14···O1	0.93	2.45	2.773 (4)	101
C—H...π Interactions				
C6—H6···Cg1	0.93	2.718	3.573	153
C12—H12···Cg2	0.93	3.047	3.802	139
C13—H13···Cg3	0.93	2.914	3.738	148

Symmetry codes: (i) *x*, −*y*+1/2, *z*−1/2; (ii) −*x*+1, *y*−1/2, −*z*+1/2; (iii) −*x*+1, −*y*+1, −*z*+1.

Table 3

Crystal parameters of ABZ–N-propanoyl anthranilic acid complex and X-ray diffraction data for the complex were summarized in table 4.

Formula	$C_7H_8N_3^+$, $C_{10}H_{10}NO_3^-$
FW	326.35
Crystal system	Monoclinic
Space group	$P2_1/c$
a (Å)	9.860 (4)
b (Å)	16.673 (2)

c (Å)	10.573 (3)
β (°)	108.13 (3)
Volume (Å^3)	1651.8 (8)
Z	4
D_x (Mg m^{-3})	1.312
Crystal size (mm)	0.45 × 0.29 × 0.19
Radiation (Å)	Ag $K\alpha$ 0.56087
Uniq. Data, R_{int}	6689, 0.031
Observed data [$I > 2.0$ sigma(I)],	4725, 219
R, wR, S	0.073, 0.227, 1.01
Min. and max. resd. dens. (e Å^{-3}),	−0.40, 0.48
$(\Delta/\sigma)_{max}$	0.001

Table 4

Out of five potential N—H hydrogen-bond donors present in the cation, there are at least 8 distinct hydrogen bonds distributed over three potential acceptors atoms. These highly directional N—H…O hydrogen bonds are the main driving force which mediate the crystal packing features of the title compound. Indeed, the donation of hydrogen atoms from the cation to the carboxylate group of an adjacent anion via N1—H1A…O2 and N2—H2…O1 (dashed orange lines in Fig. 6), forms the known structurally robust $R_2^2(8)$ graph-set motif [31-32]. This graph-set motif has previously, been found in related compounds [38-42].

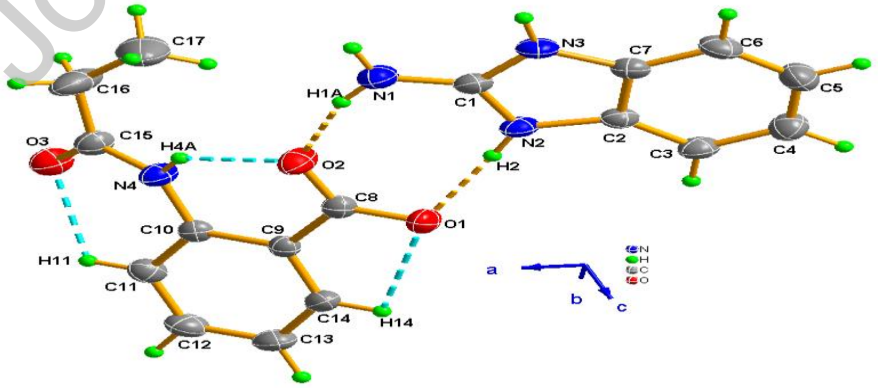

Figure 6: (a)The molecular conformation and atom-numbering scheme for the individual cation and anion species in (**1**). Displacement ellipsoids are drawn at the 30% probability level and H atoms are shown as small spheres of arbitrary radii. Inter-species hydrogen bonding is shown as dashed lines. (b) 3D-association of cation and anion species in (**1**) by

means multiple intra and intermolecular hydrogen bonds (c) View of C—H…π interactions. Non-interactive H atoms are omitted for clarity of figures.

In the crystal lattice, the cation [$C_7H_8N_3^+$] and the anion [$C_{10}H_{10}NO_3^-$] species are packed by means two moderated N1—H1A…O2 (N1…O2 = 2.764(4) Å) and N2—H2…O1 (N2…O1 = 2.756(3) Å) hydrogen bonding interactions (Fig. 6(b)). These later together with N1—H1B···O1^{i} (N1…O1i = 2.830(3) Å with (i) x, −y+1/2, z−1/2) and N3—H3A···O3^{ii} (N3…O3 = 2.722(3) Å with (ii) −x+1, y−1/2, −z+1/2) interactions extend the structure supramolecularly in 3D network (Fig. 6(b)). The packing interaction is also mediated by C—H…π interactions (Table 2, dashed yellow lines in Fig 6(c), via C6—H6…Cg1, C12—H12…Cg2 and C13—H13…Cg3 with mean H…Cg_i distance of 2.893 Å; with Cg1, Cg2 and Cg3 are the centroids of the benzene C9—C14 and C2–C7 rings and the imidazole C1–N3 ring, respectively.

With regard to the geometrical features of **1**, the COOH group of substituted benzoic acid is ionized by proton transfer to the nitrogen atom of the imidazolyl moiety, which is also confirmed by the bond distances of C8—O1, 1.252(3) Å and C8—O2, 1.262(3) Å for the carboxylate group. The weak Δ value of 0.01 Å in bond distances further verified the deprotonating of COOH group in favor of imidazole base (N2—C1, 1.329(3) Å and N2—C2, 1.400(4) Å). In the other hand, both of benzene and azolinic rings are planar as expected since the *rms* deviations from the mean planes of the rings are ± 0.006 Å for C2—C7 and ± 0.012 Å for C9—C14 benzenic rings and ± 0.013 Å for azolinic ring. The carboxylate group of the anion and the NH_2 of the cation deviated by means 11.1(2)° and 1.9(4)° from the benzene and imidazole rings, respectively, suggesting that they are almost coplanar.

The occurrence of aryl C14—H14...O1 and N4—H4A…O2 (Table 3) intramolecular hydrogen bonds well explain the coplanar arrangement between the aryl moiety and the carboxylate group.

3.4.Theoretical calculations discussions

Starting geometries were taken from X-ray refinement data. The optimized results in the free molecule state are therefore, compared to those in the crystalline state. At the optimized structure Figure. 7 of the title salt, no imaginary wave number modes are obtained, proving that the optimized geometry corresponds to true energy minimum.

The application of reactivity parameters derived from density functional theory in a local sense, in particular the softness and Fukui function, to interpret and predict the mechanisms of various organic reactions has been discussed.

Global reactivity descriptors such as chemical potential, global hardness, global softness and electrophilicity index account for the overall reactivity and stability of the studied molecules.

Reactivity trends of R1 and R2 systems have been analyzed. It is evident from the reactivity descriptors that the reactivity of these two systems follows the order R1 > R2.

From table 5, $\Delta E1$ energy difference is smaller than $\Delta E2$ therefore R2 reacts as a nucleophile, whereas R1 reacts as electrophile. The global electrophilicity ω measure the propensity of specie to accept electrons. Thus, a good nucleophile has low values of μ and ω. On the other hand, a good electrophilie is characterized by high values of μ and ω (table 4). From the values reported in Tables 5 and 6 , the reactivity order of the R1 for the electrophilic case was: C4>N7>N10. The nucleophilic reactivity order for R2 was C3>C6>C8…. From these results, we can conclude that the possibility of attack of the nitrogen on the carbonyl is to be ignored. From this study, R1 is considered as Soft Lewis acid and characterized by low energy LUMO whereas, R2 is considered as Soft Lewis base and characterized by low energy HOMO (Figure 8) (table 5). Then the reaction is obtained from acid basic reaction and the possibility of obtaining the quinazoline is not possible at the conditions of the experience.

These results qualify both hydrogen and nitrogen centers as soft centers. Again, it is consistent with the nucleic base capabilities to form O-H. . .N hydrogen bonds in the base pairs. Condensed Fukui functions were determined to identify changes in the reactivity of R1 and R2 in the gas and aqueous phases. The influence of the solvent was taken into account with the PCM model[35]. The values of Fukui functions descriptors indicated that the interaction of R1 with ethanol diminished its reactivity in comparison with the exhibited in gas phase while the reactivity of R2 in the same solvent decreases.

Table 7 lists the DFT, HF and MP2/6-31G(d) optimized bond lengths, bond angles and hydrogen bonding for the structure studied here. The highest bond length difference is 0.14 Å for the C17-C18 bond at B3LYP, HF and MP2, where the biggest bond angle deviation occurred in the C7-N1-H35 and C2-N1-H35 angle 6.0˚ in B3LYP, HF and MP2 methods. It is important to mention that there are significant differences in bond lengths and in bond angles determined with the DFT, HF and MP2 methods. The obtained results by the DFT method is very closer to the experimental one. The only differences between the theoretical calculated data and experimental one are due to the fact that the theoretical calculation are collected in gaseous phase and no molecular interactions are considered, whereas the experimental data are acquired in the solid state and crystal field interactions, e.g. Van der Waals forces, crystal packing force and hydrogen bond interactions. The observed discrepancies between the theoretical and experimental results may be attributed to different environments of the molecule, being isolated state in gas phase for theoretical study, whereas the XRD values are about the molecule in the solid state, there by subjection to the intermolecular forces, which are present into π-π, N-H···O and C-H···O interactions. The theoretical structure are stabilized by inter molecular hydrogen bond. The difference in energy between the salt product and the two reactants (N-acylanthranilic acid and 2-aminobenzimidazole) is about 16 kcal mol^{-1}.

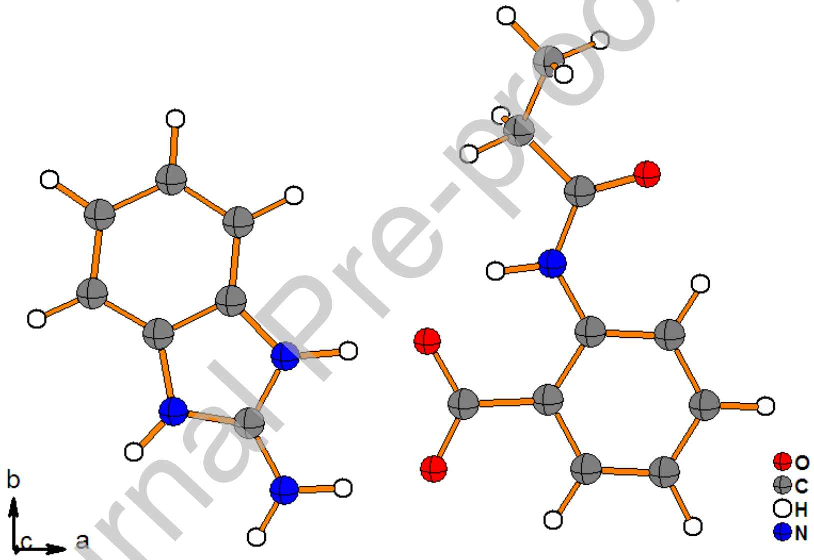

Figure 7: Structure of the title compound **1** at the B3LYP/6-31G(d) level

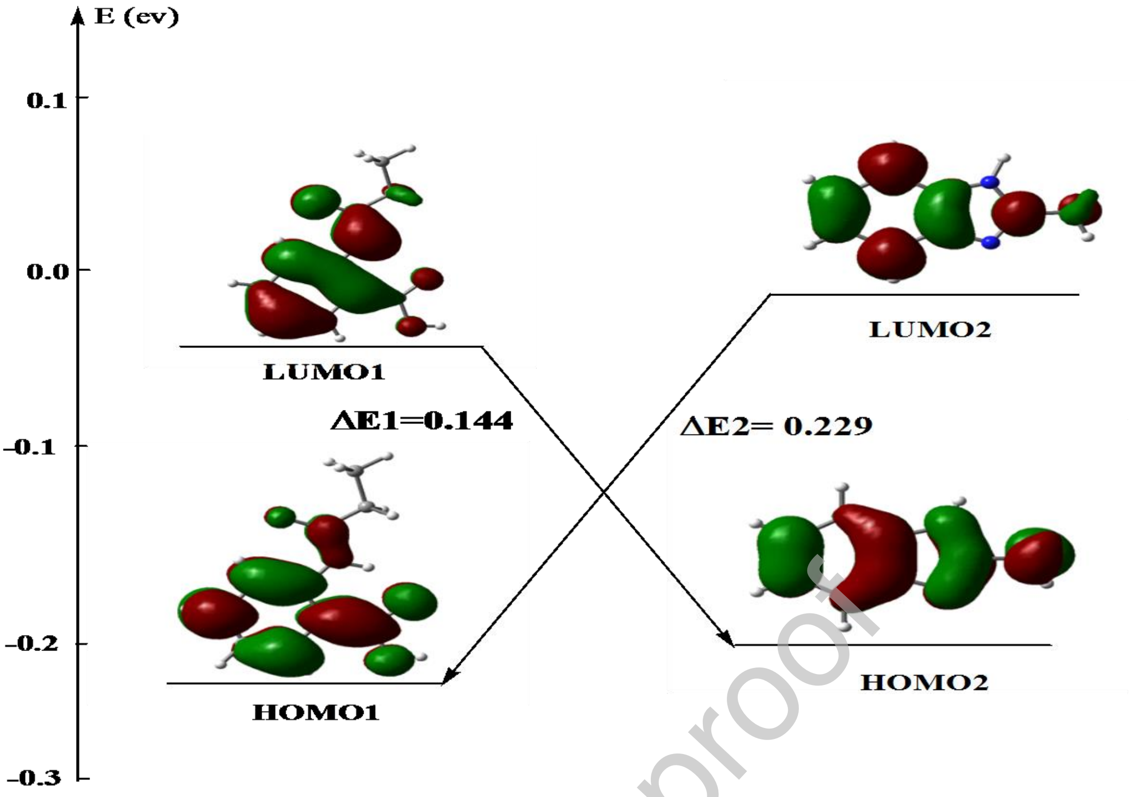

R1 : N-propanoyl anthranilic acid **R2 : 2- aminobenzimidazole**

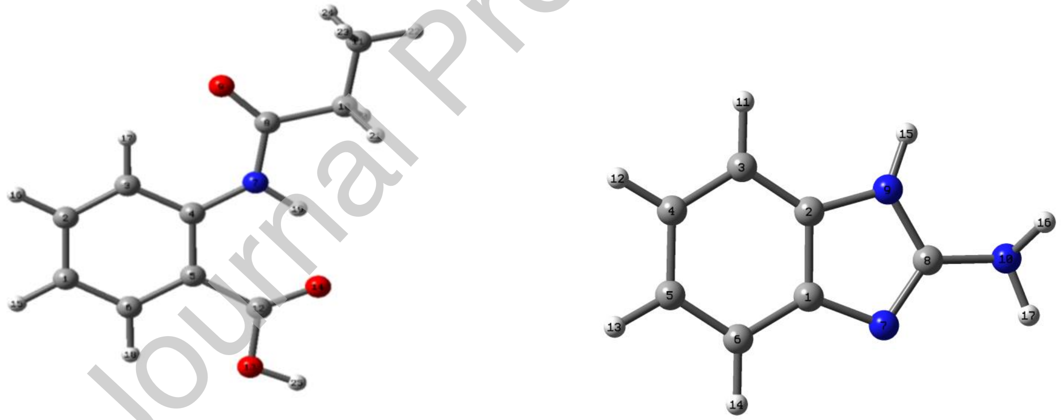

Figure 8: The atomic orbital components of the frontier molecular orbital of R1 and R2.

	E HOMO(ev)	E LUMO(ev)	S	η	μ	ω
R1	**-0.22593**	**-0.05636**	**5.896**	**0.0848**	**-0.1411**	**0.1174**
R2	**-0.20021**	**0.00350**	**4.907**	**0.1019**	**-0.0984**	**0.0475**

Table 5: Values of the Fukui function considering NBO charges for R1 and R2

R1						
atom number	**Gaz**		**Ethanol**		**Toluene**	
	Fk^-	**Fk^+**	**Fk^-**	**Fk^+**	**Fk^-**	**Fk^+**
C1	0.1652	0.0185	0.1786	0.0195	0.1738	0.0183
C2	-0.0078	0.1367	-0.0013	0.1450	-0.0038	0.1425
C3	0.0986	0.0084	0.1141	0.0190	0.1075	0.0145
C4	0.0403	0.0843	0.0652	0.0873	0.0527	0.0866
C5	0.0729	0.0429	0.0744	0.0610	0.0753	0.0529
C6	0.0272	0.0699	0.0384	0.0864	0.0331	0.0793
N7	0.1633	-0.0081	0.1589	0.0011	0.1645	-0.0030
C8	-0.0059	0.0512	0.0053	0.0393	0.0004	0.0435
C9	0.1108	0.0612	0.1049	0.0434	0.1062	0.0506
C10	-0.0101	-0.0080	-0.0053	-0.0051	-0.0064	-0.0064
C11	-0.0102	-0.0053	-0.0037	-0.0023	-0.0054	-0.0042
C12	-0.0059	0.1302	0.0017	0.1403	-0.0013	0.1356
O13	0.0233	0.0440	0.0172	0.0476	0.0202	0.0464
O14	0.0436	0.1174	0.0372	0.1168	0.0411	0.1167

R2						
atom number	**Gaz**		**Ethanol**		**Toluene**	
	Fk^-	**Fk^+**	**Fk^-**	**Fk^+**	**Fk^-**	**Fk^+**
C1	0.0710	0.0499	0.0796	0.0512	0.0851	0.0493
C2	0.0844	-0.0089	0.0959	0.0142	0.0910	0.0022
C3	0.0013	0.1574	0.0073	0.1914	0.0060	0.1724
C4	0.1726	0.0809	0.1572	0.0861	0.1613	0.0932
C5	0.0323	0.0186	0.0459	0.0317	0.0459	0.0198
C6	0.0637	0.1499	0.0595	0.1920	0.0532	0.1769
N7	0.1461	0.0091	0.1278	0.0399	0.1112	0.0439
C8	0.0583	0.1129	0.0562	0.0948	0.0613	0.1071
N9	0.0045	0.0294	0.0179	0.0184	0.0156	0.0220
N10	0.1094	0.0413	0.1388	0.0336	0.1282	0.0307

Table 6: Reactivity descriptors for R1 and R2 at the level B3LYP/6-31G(d).

		D-H...A	D-H	H...A	D...A
DFT	N(2) -H(35) ...O(2)	1.067	1.589	2.665	175.6
	N(1) -H(36) ...O(1)	1.054	1.655	2.706	174.3
	C(14)-H(14)...O(1)	1.084	2.329	2.735	100.1
	C(11)-H(11)…O(3)	1.081	2.178	2.901	122.3
	N(4)-H(37) ...O(2)	1.025	1.753	2.637	142.0
HF	N(2) -H(35) ...O(2)	1.030	1.706	2.733	175.7
	N(1) -H(36) ...O(1)	1.021	1.758	2.771	170.7
	C(14)-H(14)...O(1)	1.071	2.313	2.710	99.8
	C(11)-H(11)…O(3)	1.068	2.194	2.892	121.0
	N(4)-H(37) ...O(2)	1.001	1.805	2.652	140.1
MP2	N(2) -H(35) ...O(2)	1.046	1.709	2.745	169.9
	N(1) -H(36) ...O(1)	1.125	1.434	2.559	177.9
	C(14)-H(14)...O(1)	1.085	2.319	2.727	100.1
	C(11)-H(11)…O(3)	1.082	2.162	2.892	122.6
	N(4)-H(37) ...O(2)	1.023	1.761	2.636	141.0

Symmetry codes: (i) $-x+1, -y+1, -z+1$.

Table 7: DFT/6-31G(d), HF/6-31G(d) and MP2/6-31G(d) calculations of Hydrogen-bond lengths (Å) of the compound **1**.

4. Conclusion

Complex **1** were synthesized and characterized by spectroscopic data, by Single crystals and theoretical calculations. The structure of the compound **1** was confirmed by melting point, FT-IR, ^{1}H NMR, ^{1}H–^{1}H NOESY, ^{13}C NMR, DEPT, ^{13}C-^{1}H NMR HMQCGP, HMBCGP), elemental analysis, X-ray diffraction and theoretical calculations. This organic compound proved to be useful intermediate in heterocyclic synthesis through a straightforward intermolecular condensation. In the solid state, molecules are organized by pairs where both members are linked by intermolecular hydrogen bonds. Molecular structure of **1** shows a complete corroboration with the spectroscopic structure determination.

Credit author statement

Abir. Ben Hadj Amor : investigation writing, software, Original draft preparation.validation of organic study. **Sameh. Akriche**: visualisation and writing of X-Ray diffraction and validation of this part. **Youssef. Arfaoui** visualisation, writing of DFT calculation and validation of this part. **Raoudha. Abderrahim** : - Original draft preparation Conceptualisation, Reviewing and Editing, supervision.

Declaration of interests

☒ The authors declare that they have no known competing financial interests or personal relationships that could have appeared to influence the work reported in this paper.

Supplementary data

CCDC 982671 contains the supplementary crystallographic data for structure **1**. This data can be obtained free of charge via www.ccdc.cam.ac.uk/conts/retrieving.html (or from the Cambridge Crystallographic Data Centre, 12 Union Road, Cambridge CB2 1EZ, UK.

References

[1] Salahuddin, M. Shaharyar, A. Mazumder, Arab. J. Chem. 10 (2017) S157-S173

[2] M. Tariq Khan, M. T. Razi, S. U. Jan, M. Mukhtiar, R. Gul, I. Ullah, A. Hussain, A. M. Hashmi, M. Taufiq Ahmad, N. A. Shahwani and I. Rabbani, Pak. J. Pharm. Sci. 31 (2018) 1067-1074.

[3] E. M. E. Dokla, N. S. Abutaleb, S. N. Milik, D. Li, K. El-Baz, M. W. Shalaby, R. Al-Karaki, M. Nasr, C. D. Klein, K. A. M. Abouzid, M. N. Seleem, Eur. J. Med. Chem. 186 (2020) 111850.

[4] I. A. Dvornikova, E. V. Buravlev, I. V. Fedorova, O. G. Shevchenko, I. Y. Chukicheva and A. V. Kutchin, Russ. Chem. Bull. 68 (2019) 1000–1005.

[5]P. J. Preethi, E. Karthikeyan, M. Lohita, P. Goutham. Teja, M. Subhash, P. Shaheena, Y. Prashanth, K. Sai Nandhu, Asian J. Pharm. Tech. 5 (2015) 138-152.

[6] R. Sharma, A. Bali, B. B. Chaudhari, Bioorg. Med. Chem. Lett. 27 (13) (2017) 3007-3013.

[7] H. Y. Aboul-Enein and A. A. El Rashedy, Med. Chem. 5(7) (2015) 318-325.

[8] R. Kalirajan, L. Rathore, S. Jubie, B. Gowramma, S. Gomathy, S. Sankar and K. Elango, Indian J. Pharm. Educ. Res. 44 (2010) 358-362.

[9] I. Tamm, P. B. Sehgal, Adv. Virus. Res. 22 (1978) 163-86.

[10] I. Tamm, Science. 120 (1954) 847-848.

[11] M. M. Ramla, A. M. Omar, H. Tokudo, I. H. El-Diwoni, Bioorg. Med. Chem. 15 (2007) 6489-6496

[12] Z. Kazimierzcuk, D. Shugar, Nucleosides Nucleotides. 8 (1989) 1379-1385

[13] R. Ottana, S. Carotti, R. Maccari, I. Landini, G. Chiricosta, B. Cacigli, G. M. Vigorita, E. Mini, Bioorg. Med. Chem. Lett. 15 (2005) 3930-3933.

[14] A. Brugarolas, M. Gosalvez, Recent Results Cancer Res. 80 (1982) 346-350.

[15] A. S. Athmani, F. Madi, I. Laafifi1, M. Cheriet, N. Issaoui, L. Nouar and R. Merdes, J. Struct. Chem. 60(12) (2019) 1906-1916.

[16] D. E. Lynch, G. Smith, K. A. Byriel, C. H. L. Kennard, Aust. J. Chem. 5 (1998) 587-592.

[17] D. E. Lynch, C. J. Cooper, V. Chauhan, G. Smith, P. Healy, S. Parsons, Aust. J. Chem. 52 (1999) 695-697.

[18] D. E. Lynch, L. J. Nicholls, G. Smith, K. A. Byriel, C. H. L. Kennard, Acta. Cryst. B55 (1999) 758-766.

[19] Q. Shou, L. K. Banbury, A. T. Maccarone, D. E. Renshaw, H. Mon, S. Griesser, H. J. Griesser, S. J. Blanksby , J. E. Smith , H. Wohlmuth, Fitoterapia. 93 (2014) 62-66.

[20] J. D. Patrone, N. F. Pelz, B. S. Bates, E. M. Souza-Fagundes, B. Vangamudi, D.V. Camper, A. G. Kuznetsov, Carrie F. Browning, M. D. Feldkamp, A. O. Frank, B. A. Gilston, E. T. Olejniczak, O. W. Rossanesea, A. G. Watersonb, W. J. Chazina,, and S. W. Fesika, Chem. Med. Chem. 11(8) (2016) 893–899.

[21] A. Nina, A. Tavani, Z. Iran, J. Chem. Chem. Eng. 37(5) 2018 47-54.

[22] Q. Qin, J. T. Mague, H. E. Gould, S. E. Vasquez and A. E. Heyer, Acta. Cryst E 75 (2019) 1573-1577.

[23] S. Amirat, F. Madi, M. Bououdina, A. Gheid, A. Zaboub, L. Nouar and R. Merdes, Mater. Res. Express. 6 (2019) 075104-24.

[24] P. Singh, P. Kumar, R. Kalra, S. K. Dass, S. Prakash, R. Chandra, Spectrochim. Acta A. 75 (2010) 983-991.

[25] S. M. Teleb, A. S. Gaballa, M. A. F. Elmosallamy, E. M. Nour, Spectrochim. Acta. A. 61 (2005) 2708-2712.

[26] G. Smith, Urs. Wermuth, P. C. Healy, Acta. Cryst. C63 (2007) o405-o407.

[27] J. Jones, V. Ta. Phuoc, L. Del Campo, N. E. Massa, C. M. Brown, S. Pagola, Cryst. Growth. Des. 9 (2019) 4970-4980.

[28] T. J. Wasowicz, M. Łabuda, and B. Pranszke, Int. J. Mol. Sci. 20 (2019) 6022-20.

[29] M. S. Khajavi, N. Montazari, S. S. S. Hosseini, J. Chem. Res. 8 (1997) 286-287.

[30] W. M. Welch, F. E. Ewing, J. Huang, F. S. Menniti, M. J. Pagnozzi, P. A. S. K. Kelly, V. Guanowsky, S. Guhan, M. R. Guinn, D. Critchett, J. Lazzaro, A. H. Ganong, K. M. DeVries, T. L. Taigers, B. L. Chenard, Bioorg. Med. Chem. Lett. 11 (2001) 177-182.

[31] G. M. Sheldrick, SHELXS-97. Program for Crystal Structure Solution (University of Göttingen, Germany, 1997).

[32] M. J. Frisch, G. W. Trucks, H. B. Schlegel, Gaussian 09, Revision A1, Inc., Wallingford CT, (2009).

[33] A. D. Becke, J. Chem. Phys. 98 (1993) 5648-5652.

[34] C. Lee, W. Yang, R. G. Parr, Phys. Rev. 37 (1988) 785-789.

[35] R.G. Parr, R. G. Pearson, J. Am. Chem. Soc. 105 (1983) 7512-7516.

[36] P.W. Ayers, R. G. Parr, R. G. Pearson, J. Chem. Phys. 124 (2006) 194107-194107-8.

[37] R. G. Parr and V. Szentpály, J. Am. Chem. Soc. 121 (1999) 1922-1924.

[38] Y. Arfaoui, M. L. Efrit and N. Besbes, J. Mol. Model. 19 (2013) 4603-4612.

[39] M. C. Etter, Acc. Chem. Res. 23 (1990) 120-126.

[40] J. Grell, J. Bernstein and G. Tinhofer, Acta. Cryst. B55 (1999) 1030–1043.

[41] S. Jin, J. Guo, L. Liu, D. Wang, J. Mol. Struct. 1004 (2011) 227-236.

[42] A. C. Kathalikkattil, S. Damodaran, K. K. Bisht, E. Suresh, J. Mol. Struct. 985 (2011) 361-370.

A novel organic reaction leading to new 2-N-substituted benzoic acid ion-pair. A combination of physicochemical and theoretical calculations approaches.

Abir. Ben Hadj Amor, Sameh. Akriche. [b], Youssef. Arfaoui [c] and Raoudha. Abderrahim [a]

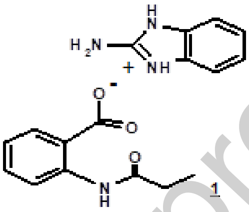

1

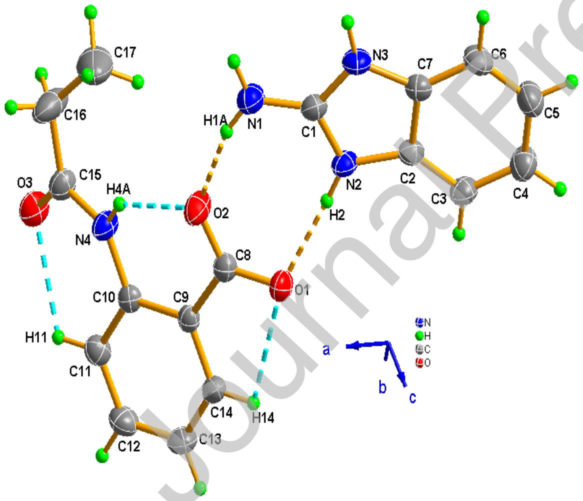

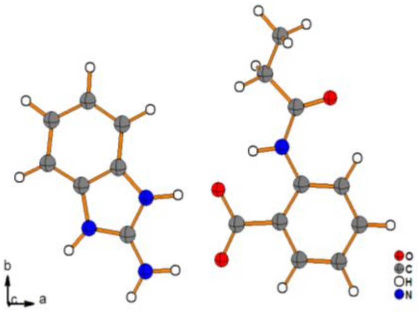

graphical abstract